



National Authority for Remote Sensing and Space Sciences  
**The Egyptian Journal of Remote Sensing and Space Sciences**

www.elsevier.com/locate/ejrs  
www.sciencedirect.com



RESEARCH PAPER

# Monitoring olive mills waste disposal areas in Crete using very high resolution satellite data



Athos Agapiou<sup>a,b,\*</sup>, Nikos Papadopoulos<sup>a</sup>, Apostolos Sarris<sup>a</sup>

<sup>a</sup> *Laboratory of Geophysical-Satellite Remote Sensing & Archaeo-environment, Institute for Mediterranean Studies, Foundation for Research & Technology, Hellas (F.O.R.T.H.), Greece*

<sup>b</sup> *Department of Civil Engineering and Geomatics, Faculty of Engineering and Technology, Cyprus University of Technology, 2-6, Saripolou str., 3603 Limassol, Cyprus*

Received 30 September 2015; revised 1 March 2016; accepted 6 March 2016

Available online 25 March 2016

## KEYWORDS

Olive mill disposal areas;  
Remote sensing;  
Very high resolution images;  
Crete

**Abstract** This paper evaluates the efficiency of different image analysis techniques applied to high resolution multispectral satellite data so as to identify olive oil waste disposal areas in the island of Crete where huge quantities of wastes are produced. For this purpose very high spatial resolution images including Pleiades, SPOT 6, QuickBird, WorldView-2 and GeoEye 1 have been exploited. The research included the application of the Normalised Difference Vegetation Index, Olive Oil Mill Waste Index as well as Principal Component Analysis. Moreover Intensity–Hue–Saturation transformation was carried out. Furthermore, unsupervised classification was performed for a variety of classes (5; 10 and 15) over the same area for two different periods. In addition, supervised linear constrained spectral un-mixing technique has been applied for the WorldView-2 image, to evaluate the potential use of sub-pixel analysis. Indeed, as it is demonstrated NDVI and OOMW indices may be used to enhance the exposure of disposal areas in high resolution satellite datasets, while the application of the PCA and HIS transformations seems to be able to further improve the results. Unsupervised classification techniques, with no ground truth data, can sufficiently work; however temporal changes of the disposal areas can affect the performance of the classifier. The use of spectral library was able to detect OOMW areas with a relatively high rate of success improving the results from the unsupervised classification. Finally, a COSMO-SkyMed radar image has been examined and fused with a hyperspectral EO-ALI image, indicating that such kind of datasets might be also explored for this purpose.

© 2016 National Authority for Remote Sensing and Space Sciences. Production and hosting by Elsevier B.V. This is an open access article under the CC BY-NC-ND license (<http://creativecommons.org/licenses/by-nc-nd/4.0/>).

\* Corresponding author at: Department of Civil Engineering and Geomatics, Faculty of Engineering and Technology, Cyprus University of Technology, 2-6, Saripolou str., 3603 Limassol, Cyprus.

E-mail addresses: [athos.agapiou@cut.ac.cy](mailto:athos.agapiou@cut.ac.cy) (A. Agapiou), [nikos@ims.forth.gr](mailto:nikos@ims.forth.gr) (N. Papadopoulos), [asaris@ret.forthnet.gr](mailto:asaris@ret.forthnet.gr) (A. Sarris).

Peer review under responsibility of National Authority for Remote Sensing and Space Sciences.

<http://dx.doi.org/10.1016/j.ejrs.2016.03.003>

1110-9823 © 2016 National Authority for Remote Sensing and Space Sciences. Production and hosting by Elsevier B.V.

This is an open access article under the CC BY-NC-ND license (<http://creativecommons.org/licenses/by-nc-nd/4.0/>).

## 1. Introduction

Olive oil industry is very important in Mediterranean countries, both in terms of wealth and tradition and it is considered to be as one of the driving sectors of the agricultural economy of the Mediterranean basin. The annual production in the Mediterranean region is estimated up to  $2600 \times 10^3$  tones (International Olive Council), whilst Greece to third world after Spain and Italy (Asfi et al., 2012; Roig et al., 2006).

However, the production process of olive oil may cause significant environmental problems since olive processing produces large amounts of solid waste and wastewater with high organic load and rich inorganic constituents (Dermeche et al., 2013; Doula et al., 2014; Alexakis et al., 2016; Peikert et al., 2015; Pavlidou et al., 2014). For instance, uncontrolled land disposal of olive oil mill waste water (OOMW) can potentially result in soil pollution as a consequence of its high chemical and biochemical oxygen demand in addition to high concentration of phytotoxic phenolic compounds (Peikert et al., 2015). In addition, several studies have shown the negative impact of oil wastes on soil microbial populations (Paredes et al., 1987) or on aquatic ecosystems (Dellagrecia et al., 2001). Inappropriate disposal of olive husk and olive mill wastewater creates environmental problems such as odour and ammonia released into the atmosphere and leaching of inorganic and organic substances to the soil as well as leaching of these pollutants into the ground water (Rodis et al., 2002).

Therefore, as Bailey et al. (2002) argue safe disposal of wastes is very important with our culture, since we can no longer simply throw things away in random locations. Remote sensing technologies have been widely used as a systematic tool for mapping land use and land cover changes (Hegazy and Kaloop, 2015; Rawat and Kumar, 2015). Information on land use/cover and possibilities for their optimal use is essential for the selection, planning and implementation of land use

schemes to meet the increasing demands for basic human needs and welfare (Rawat and Kumar, 2015). Remote sensing images have been exploited in the last years for environmental application (Hegazy and Effat, 2010; El-Asmar et al., 2013) as an effort to detect and map olive oil waste disposal areas (Alexakis et al., 2016; Agapiou et al., in press, 2015). The results of these studies suggest that multispectral satellite data as well as spectral libraries can be used sufficiently as a systematic tool for monitoring olive oil disposal areas.

In the island of Crete, the management of olive oil waste disposal areas remains a critical and unsolved problem, especially in regions where huge quantities of wastes are produced. The aim of this study is to evaluate a variety of remote sensed data that could be used to monitor the olive mills waste water disposal areas using known image techniques. For this task the paper aims to investigate further the potential use of very high resolution satellite images for their capability to detect such areas. A variety of post-processing techniques have been applied including vegetation indices; PCA and IHS transformations, as well as classification analysis.

## 2. Methodology and resources

### 2.1. Study area

For the aims of this paper the island of Crete was selected as a case study. During the last quarter of the century, olive groves have expanded constantly in many semi-mountainous and coastal areas mainly in Crete and Peloponnese (Camarsa et al., 2010). Crete, located in the southern part of the Aegean Sea, is the fifth largest island of the Mediterranean Sea, and the largest island of Greece (Fig. 1). Crete spans 260 km from east to west while its widest point is around 60 km. Crete covers an area of approximately 8336 square kilometres while the climate

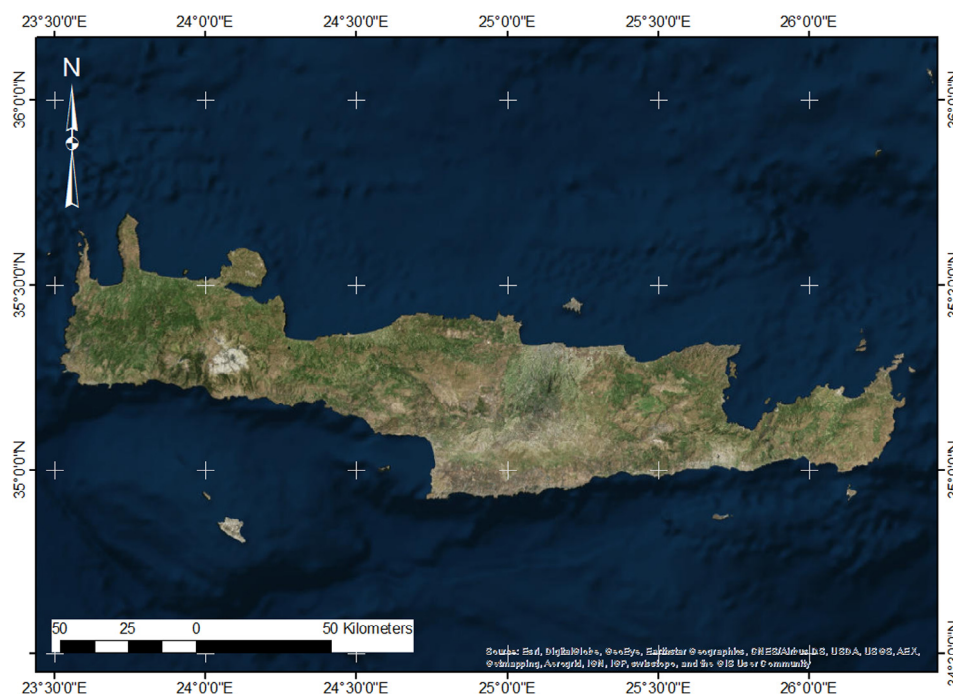


**Figure 1** The island of Crete used as a case study. In this island more than 1000 OOWM disposal areas have been recorded.

**Table 1** Characteristics of the very high resolution satellite data used in the current study.

No	Sensor	Satellite overpass	Spatial resolution (pansharpen)	Spectral resolution
1	GeoEye 1	16 July 2013	0.4 m	RGB–VNIR
2	GeoEye 1	17 May 2014	0.4 m	RGB–VNIR
3	QuickBird	21 August 2013	0.6 m	RGB–VNIR
4	WorldView 2	05 March 2013	0.4 m	RGB–VNIR
5	SPOT 6	07 October 2014	1.5 m	RGB–VNIR
6	Pleiades	15 July 2014	0.5 m	RGB–VNIR
7	Hyperion	17 March	30 m	RGB–VNIR
8	COSMO-SkyMed	30 March 2015	2.5 m	Radar

in Crete is primarily Mediterranean. Agriculture also plays a significant role for Crete and olive industry is very important for the local economy. In the island of Crete, more than 1000 OOMW disposal areas using Global Navigation Satellite Systems (GNSS) and Geographical Information Systems (GIS) have been recorded in the past.

### 2.2. Satellite sensors

For the aims of the study several very high resolution images have been exploited, with a spatial resolution ranging from 0.4 m to 1.5 m. The spectral resolution of the images was limited to the range of the visible (RGB) and VNIR part of the spectrum. The images have been acquired during the last couple of years (2013–2015). The dataset included Pleiades (0.50 m), SPOT 6 (1.5 m), QuickBird (0.60 m), WorldView-2

(0.40 m) and GeoEye 1 (0.40 m) satellite data. Table 1 provides the details for the satellite dataset, while Fig. 2 presents some typical olive oil waste disposal areas. In addition, a high resolution e-GEOS COSMO-SkyMed radar image, taken on 30th of March in 2015, was evaluated as a first attempt to investigate the potential use of such images. Fusion with EO-ALI image (17 March 2006) was also performed. The datasets selected covered almost all year, not limited into the periods just after the oil extraction, so as to evaluate also the temporal resolution of the images.

### 2.3. Image processing

The data have been processed using a variety of well-known remote sensing image analysis algorithms. In detail, the Normalised Difference Vegetation Index (NDVI) was applied to

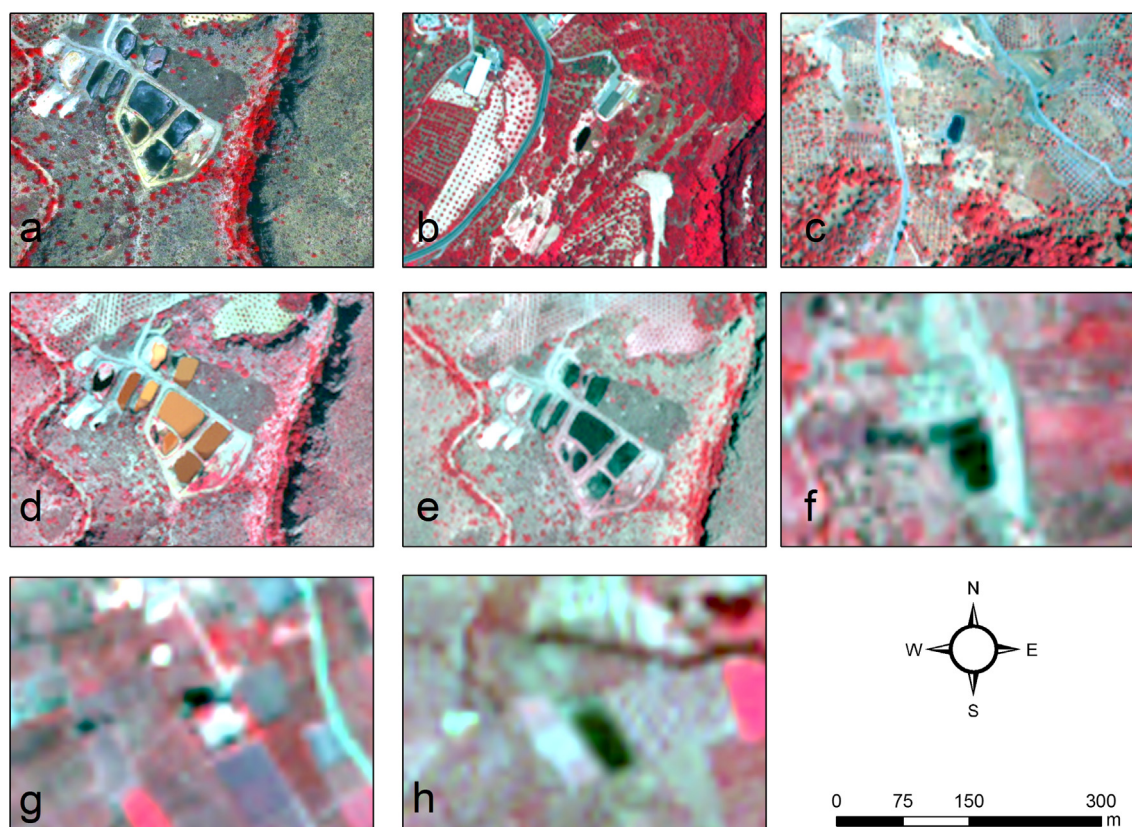


**Figure 2** Olive oil waste disposal areas shown as black target in the false composite VNIR-R-G using (a) GeoEye 1 image (16/07/2013); (b) GeoEye 1 image (17/05/2014); (c) QuickBird image (21/08/2013); (d) WorldView-2 image (05/03/2013); (e) Pleiades image (15/07/2014) and (f–h) SPOT 6 images (07/10/2014).

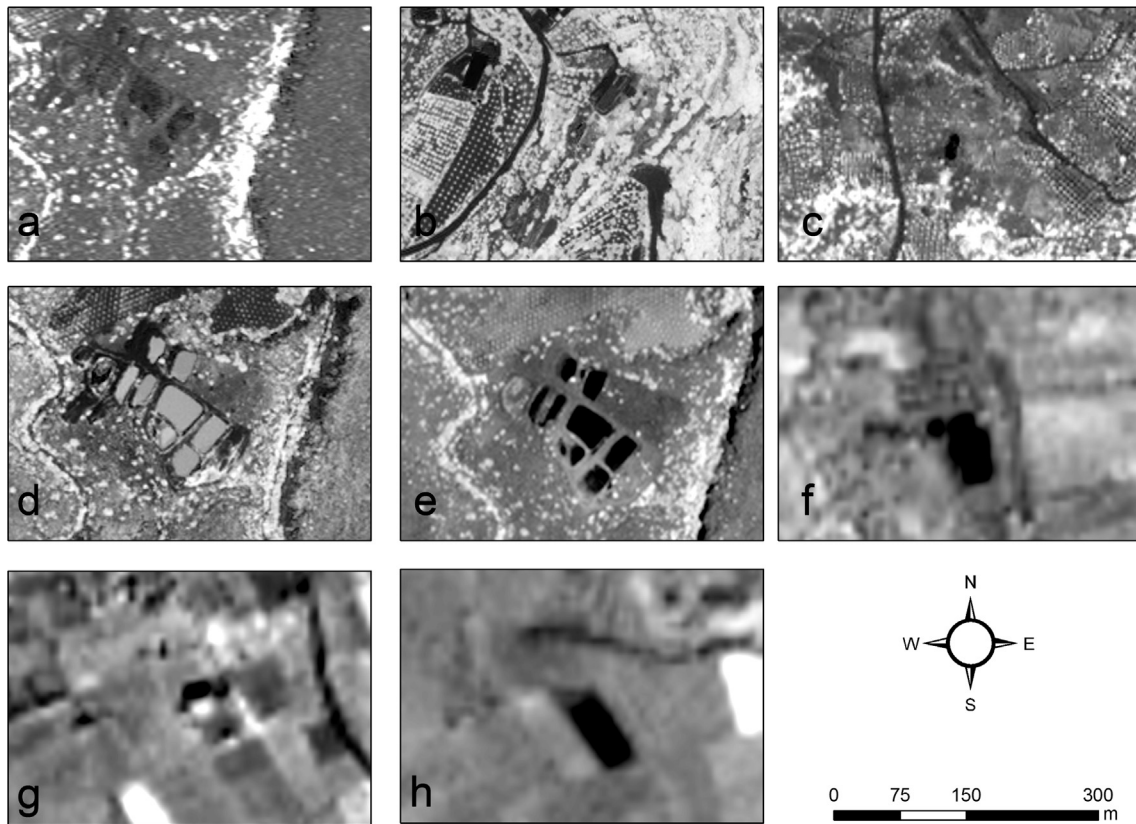


**Figure 3** Olive oil waste disposal areas shown after the application of the NDVI using (a) GeoEye 1 image (16/07/2013); (b) GeoEye 1 image (17/05/2014); (c) QuickBird image (21/08/2013); (d) WorldView-2 image (05/03/2013); (e) Pleiades image (15/07/2014) and (f–h) SPOT 6 image (07/10/2014).

all images based on Eq. (1) (Agapiou et al., 2012). NDVI is the normalised ratio of red and near infrared reflectance and is widely used in remote sensing application as a proxy for terrestrial vegetation growth because it is closely correlated with the fraction of photosynthetically active radiation absorbed by plant canopies, Leaf Area Index (LAI), potential photosynthesis and biomass (Zhang et al., 2013).

$$(p_{VNIR} - p_{red}) / (p_{VNIR} + p_{red}) \quad (1)$$

where  $p_{VNIR}$  = reflectance in the VNIR part of the spectrum,  $p_{red}$  = reflectance in the red part of the spectrum.

In addition the normalised Olive Oil Mill Waster Index (OOMW), recently proposed by Agapiou et al. (2015b), was also applied based on Eq. (2). As it was found from discriminant analysis of several ground truth spectroradiometric data, the spectral regions of 450 nm and 900 nm are the most suitable to detect of olive oil waste disposal areas. Therefore using these spectral regions (i.e. blue and VNIR bands of the multi-spectral data) such disposal areas can be better enhanced than any other spectral combination (Agapiou et al., 2015b).

$$(p_{VNIR} - p_{blue}) / (p_{VNIR} + p_{blue}) \quad (2)$$

where  $p_{VNIR}$  = reflectance in the VNIR part of the spectrum,  $p_{blue}$  = reflectance in the blue part of the spectrum.

Principal Component Analysis (PCA) was also tested in the whole dataset. In essence, PCA identifies the optimum linear combinations of the original bands that can account for vari-

ation of pixel values within an image (Campbell, 2007) as demonstrated in Eq. (3).

$$C_1 = b_{11}(X_1) + b_{12}(X_2) + \dots + b_{1p}(X_p) \quad (3)$$

where  $C_1$  = the subject's score on principal component 1 (the first component extracted).  $b_{1p}$  = the regression coefficient (or weight) for observed variable  $p$ , as used in creating principal component 1.  $X_p$  = the subject's score on observed variable  $p$ .

The Intensity–Hue–Saturation (IHS) transformation (Tu et al., 2001) was another technique applied to the satellite dataset. Intensity is related to the total brightness of a colour, while Hue refers to the dominant or average wavelength of light contributing to a colour and Saturation specifies the purity of colour relative to grey. One common IHS transformation is based on a cylinder colour model which is described by the Eqs. (4–6).

$$\begin{pmatrix} 1 \\ v1 \\ v2 \end{pmatrix} = \begin{bmatrix} \frac{1}{\sqrt{3}} & \frac{1}{\sqrt{3}} & \frac{1}{\sqrt{3}} \\ \frac{1}{\sqrt{6}} & \frac{1}{\sqrt{6}} & \frac{-2}{\sqrt{6}} \\ \frac{1}{\sqrt{2}} & \frac{-1}{\sqrt{2}} & 0 \end{bmatrix} \begin{pmatrix} R \\ G \\ B \end{pmatrix} \quad (4)$$

$$H = \tan^{-1} \frac{v1}{v2} \quad (5)$$

$$S = \sqrt{v1^2 + v2^2} \quad (6)$$

where  $v1$  and  $v2$  are two intermediate values.

Finally classification techniques using the ISODATA algorithm (Campbell, 2007) for a variety of classes (5; 10 and 15

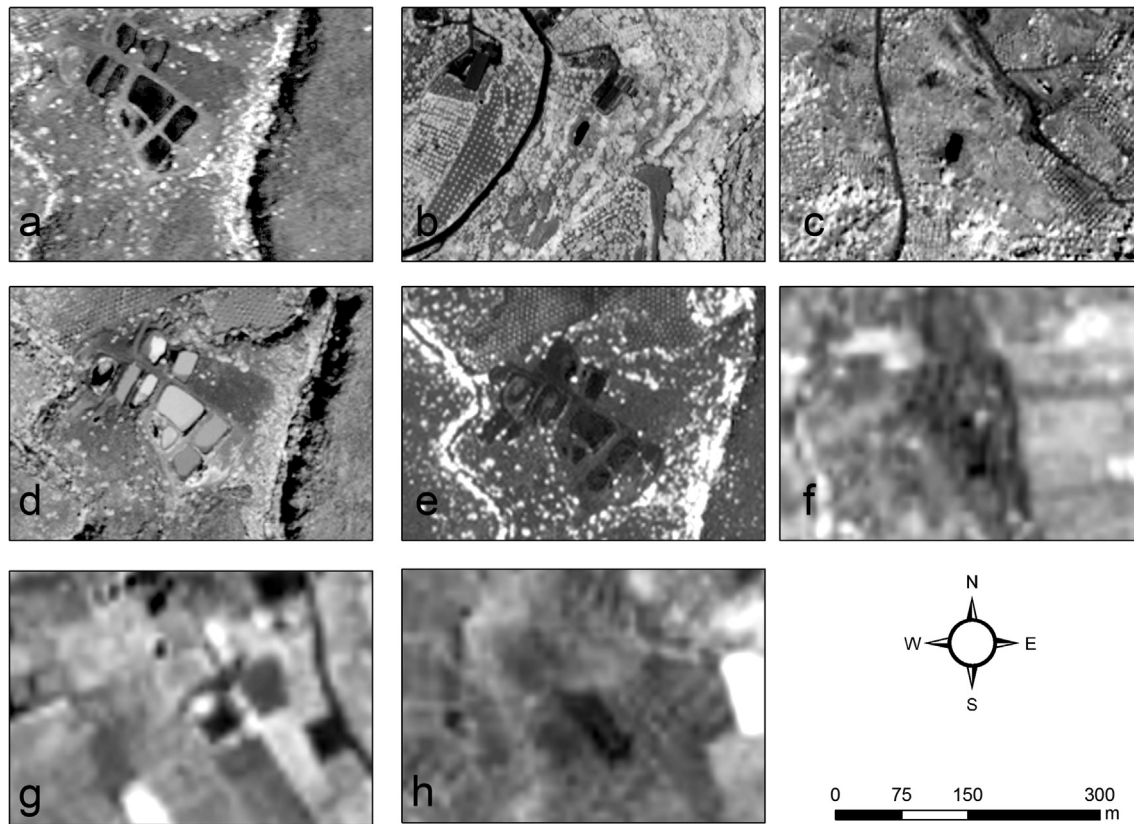


**Figure 4** Olive oil waste disposal areas shown after the application of the OOMW using (a) GeoEye 1 image (16/07/2013); (b) GeoEye 1 image (17/05/2014); (c) QuickBird image (21/08/2013); (d) WorldView-2 image (05/03/2013); (e) Pleiades image (15/07/2014) and (f–h) SPOT 6 image (07/10/2014).

classes) as well as constrained Linear Spectral Unmixing (LSU) classification were applied. LSU was used (Eqs. (7) and (8)) so as to determine the relative abundance of OOMW disposal areas that are depicted in multispectral images based on the materials' spectral characteristics. Spectral un-mixing is applied to decompose the measured spectrum of a mixed pixel into a collection of constituent spectra, or endmembers, and a set of corresponding fractions, or abundances, that indicate the proportion of each endmember present in the pixel.

$$R_k = \sum_i^n a_i E_{i,k} + \varepsilon_k \quad (7)$$

$$\text{RMSE} = \sqrt{\left( \sum_k^m \varepsilon_k^2 \right)^{-m}} \quad (8)$$

where  $R_k$  = reflectance at wavelength  $k$ ,  $E_{k,i}$  = reflectance of endmember  $i$  at wavelength  $k$ ,  $a_i$  = abundance of endmember  $i$ ,  $\varepsilon_k$  = error at wavelength  $k$ , RMSE = Root mean square error of the  $\varepsilon_k$ ,  $n$  = number of endmembers,  $m$  = number of wavelengths in the discrete spectrum.

Finally, in regard to the COSMO-SkyMed radar image, ortho-rectification was carried out using the SRTM DEM data, while other pre-processing corrections have been also carried out (speckle removal; radiometric correction etc). The COSMO-SkyMed image was then fused with a hyperspectral EO-ALI image. The images were then inserted into a GIS

platform for direct comparison with known olive oil waste disposal areas.

### 3. Results

#### 3.1. NDVI and OOMW indices

Figs. 3 and 4 show the results after the application of the NDVI and the OOMW indices. It becomes obvious that olive oil waste disposal areas can be recognised in the majority of the satellite images as black targets due to the low value of either NDVI (i.e.  $-0.30$ – $0.10$ ) or OOMW indices (i.e.  $0.20$ – $0.50$ ). Indeed, the majority of the images tend to give positive results in terms of detection of olive oil waste disposal areas. OOMW index tends to enhance better the disposal areas, contrary to the NDVI with the exception to the SPOT 6 and the Pleiades images. QuickBird 1 (Figs. 3c and 4c), Worldview (Figs. 3d and 4d) and Pleiades (Figs. 3e and 4e) seem to give the most promising results via the computation of both indices.

It is also interesting to note the temporal changes of the olive oil waste as indicated in GeoEye (Figs. 3a and 4a) and WorldView-2 (Figs. 3e and 4e) images. In general, the success of discrimination of the OOMWs depends critically on the time of acquisition of the images rather than the spatial or spectral capabilities of the sensors. This is due to the seasonal activities related with olive oil extraction and therefore

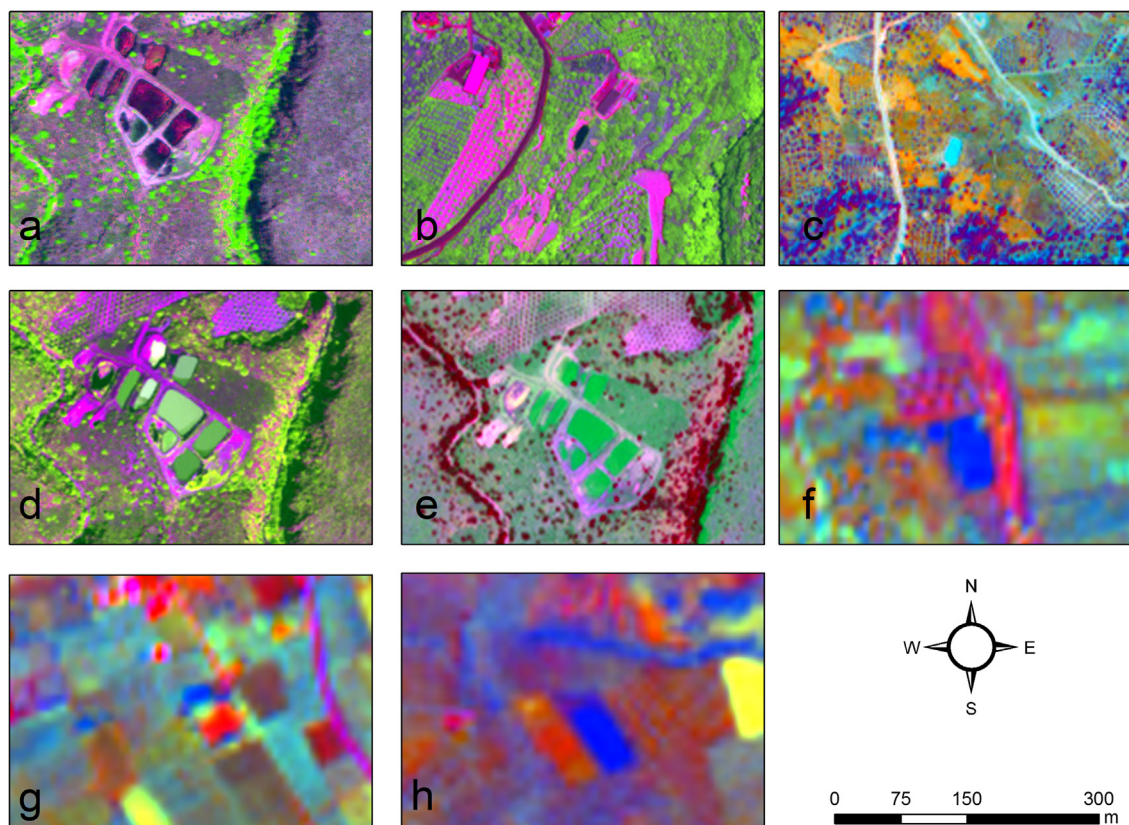


**Figure 5** Olive oil waste disposal areas shown after the application of the PCA analysis using (a) GeoEye 1 image (16/07/2013); (b) GeoEye 1 image (17/05/2014); (c) QuickBird image (21/08/2013); (d) WorldView-2 image (05/03/2013); (e) Pleiades image (15/07/2014) and (f–h) SPOT 6 image (07/10/2014).

OOMW disposal areas are more likely to be observed a couple of months after November–December rather than other period.

### 3.2. PCA and HIS transformations

In addition to the vegetation indices, Principal Component Analysis (PCA) analysis has been carried out. Fig. 5 (top) presents the pseudo-colour composite from the first three principal components PC (PC1 with Red; PC2 with Green and PC3 with Blue colours), while Fig. 5 (bottom) shows only the first principal component (PC1). It is evident that PCA analysis can improve the interpretation of the results of the satellite data related with the detection of olive oil waste disposal areas. The first PC (Fig. 5, bottom) was able to enhance the interpretation of all disposal areas (indicated as black targets), even compared to the poor result of the NDVI regarding the SPOT 6 or GeoEye 1 image. Although PC analysis is expected to provide different results for each dataset, since it considers the covariance matrix of each image under investigation, in this case the PCA was able to recover the spectral information related with the disposal areas in the whole dataset.

Detection of OOMW disposal areas was improved after the application of the IHS transformation. As shown in Fig. 6, the results are able to support interpretation of the data so as to detect olive oil waste disposal areas. These areas are coloured as green areas, compared to red and blue colours for vegetation and soil classes respectively and with the use of other

interpretation keys, such as the rectangular shape of the disposal areas can assist the user to detect such targets in the satellite images.

### 3.3. Unsupervised and LSU classification

The ISODATA unsupervised classification technique was assessed for images taken under different periods. Both WorldView-2 (05/03/2013) and Pleiades (15/07/2014) images have been examined. The ISODATA algorithm was set to maximum 6 iterations with 95% threshold, while the numbers of classes were set to 5; 10 and 15. Fig. 7 presents the final results after the classification of the images. For the Pleiades image, the class related with the olive oil disposal areas was coloured as black. As it is shown, the ISODATA algorithm was capable to detect the disposal areas in the Pleiades dataset for the variety of the different number of classes. In fact although the number of the classes was rising from 5 to 15 the disposal areas have not misclassified (Fig. 7d, f and h). Some false true results can be seen in the eastern part of the image which is linked however with the shadowed sections of the image. In contrast, the results were found relatively poor for the WorldView-2 image. Even for a small number of classes (Fig. 7c) the olive oil disposal areas were misclassified while the results are even worse for 10 and 15 classes (Fig. 7e and g respectively). Indeed, as it is shown the temporal changes of the olive oil wastes from fresh liquid to relatively dry residues can affect the performance of the unsupervised ISODATA classification.

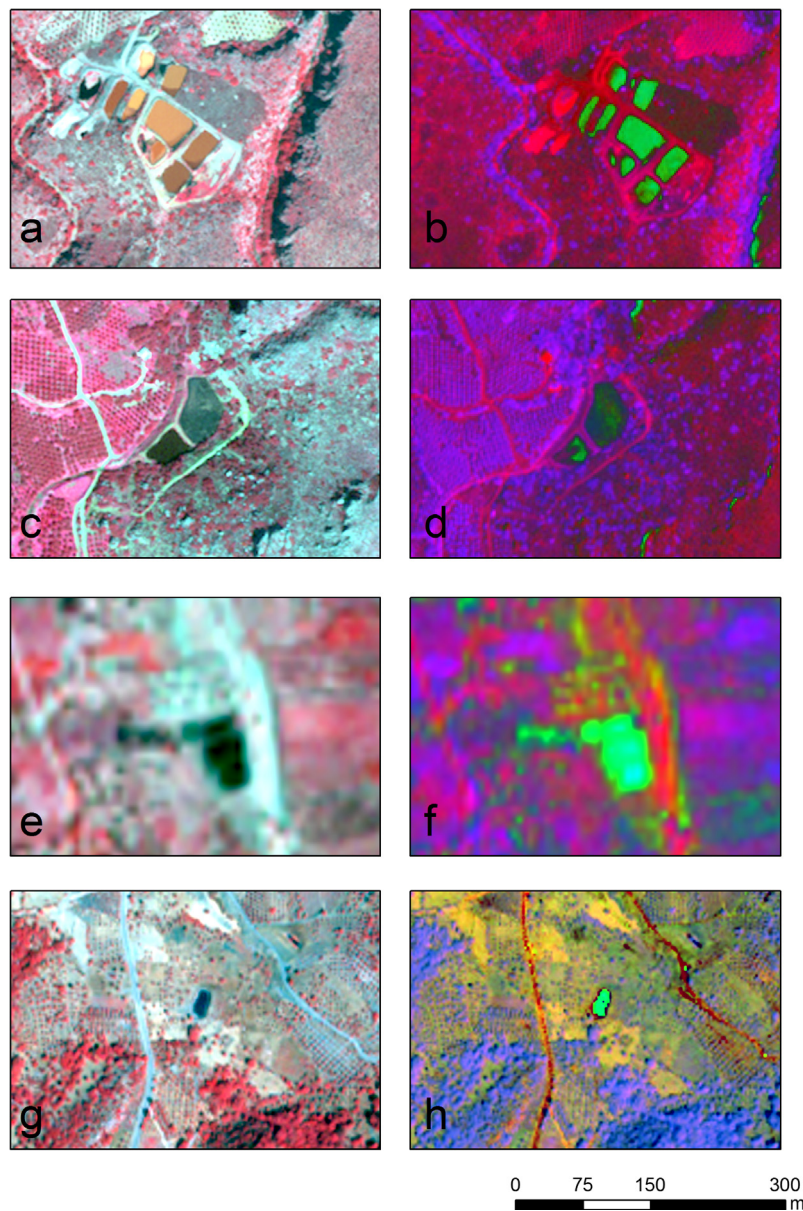


**Figure 6** Olive oil waste disposal areas shown after the application of the HIS transformation analysis using (a and b) WorldView-2 image (05/03/2013); (c and d) Pleiades image (15/07/2014); (e and f) SPOT 6 image (07/10/2014) and (g and h) QuickBird image (21/08/2013).

In order to enhance the classification results for the WorldView-2 image, the constrained LSU technique (see Eqs. (7) and (8)) was applied using the spectral signatures of the OOMW areas and the results are demonstrated in Fig. 8. In detail, Fig. 8b–e presents the abundance maps for olive oil waste disposal areas, vegetated areas, white and dark soil respectively. Red colour indicates higher abundance for each endmember while blue colours lower values. As presented in Fig. 8b the use of spectral library was able to detect the olive oil waste disposal area with a relatively high rate of success (red colour) improving the results from the unsupervised ISO-DATA classification as discussed above. For the rest of the abundance maps (Fig. 8c–e), olive oil waste disposal areas were mapped with a small percentage of endmember, indicat-

ing that the spectral signature of the OOMW disposal areas is quite dissimilar from the vegetation and soil targets.

#### 3.4. Radar analysis

Further to the very high resolution optical data, a first attempt to assess the capability of high resolution (2.5 m) COSMO-SkyMed radar image was implemented. The initial image was ortho-rectified using the SRTM DEM, while the radiometric correction and speckle removal algorithms were also applied in the Sentinel-1 toolbox of ESA. Fig. 9 presents the results from the radar image over two known olive oil waste disposal areas in the southern part of Crete. Due to the content

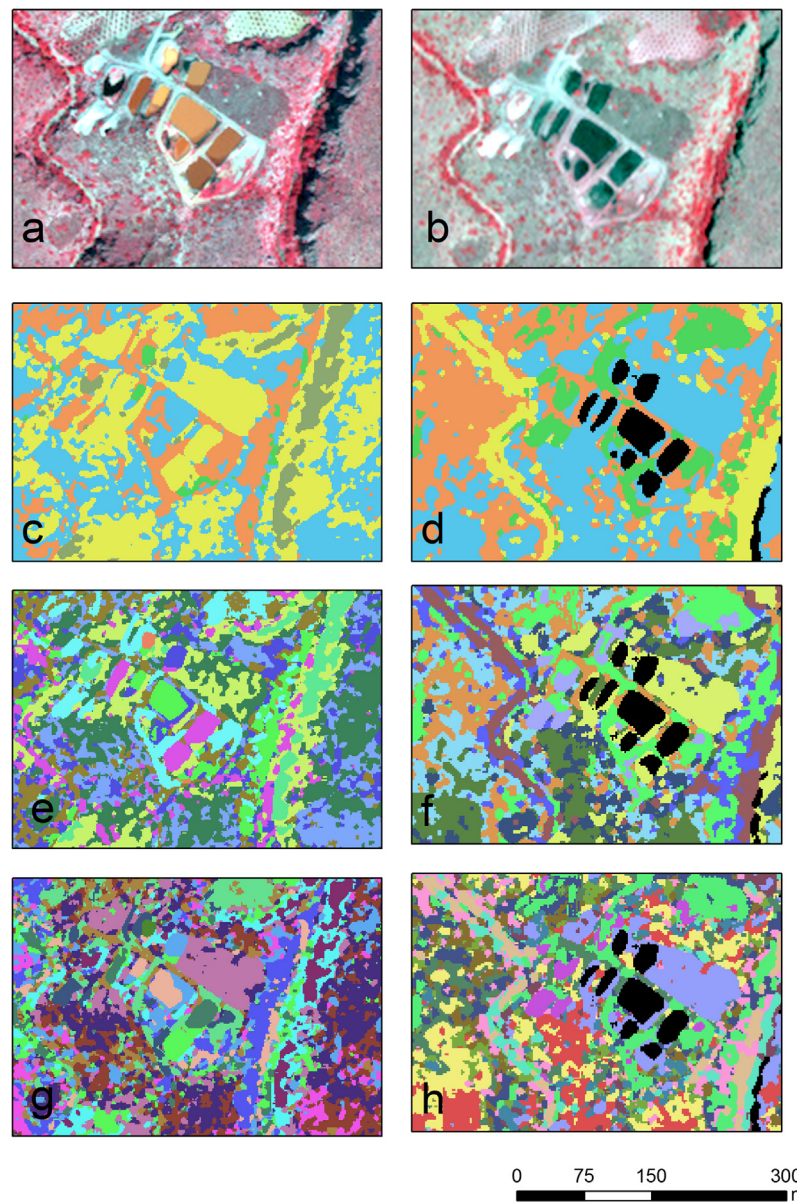


**Figure 7** Olive oil waste disposal areas shown after the unsupervised classification analysis (ISODATA) for WorldView-2 image (05/03/2013) (a) and Pleiades image (15/07/2014) (b) for 5 (c and d); 10 (e and f) and 15 (g and h) classes respectively.

of water the disposal areas are indicated as black targets, due to low backscattering of the signal. This characteristic can be further exploited in radar images (same as the behaviour of open air water reservoirs) so as to identify olive oil waste disposal areas, even in cloud covered areas. The potential use of radar images to penetrate clouds can be used in cases where the analysis of optical images is poor due to high percentage of cloud cover.

In addition, a hyperspectral EO-ALI image (30 m spatial resolution) covering the same area was used through fusion techniques with the COSMO-SkyMed image. Fig. 10 (top) presents the false composites 9-7-5 and 8-5-3 of the hyperspectral image and Fig. 10 (bottom) the fusion results based on multiplicative transformation. Even if the fused images have an improved spatial resolution, they have not been extremely successful in distinguishing the olive oil waste disposal areas.

#### 4. Discussion

In this study different remote sensing datasets and algorithms have been applied so as to evaluate their capabilities for recording OOMW disposal areas in Crete Island. As it was found regarding the satellite datasets, both optical and radar images are capable to enhance and detect disposal areas. It has been demonstrated that both spatial and temporal resolution of the datasets are critical for the detection of these areas. Indeed, the spectral signature of the OOMW disposal areas is changing through the year and therefore their detection might be problematic in some periods (e.g. see NDVI and OOMW index for SPOT). The impact of spatial resolution for the detection of OOMW disposal areas was observed in the application of the fusion of radar COSMO-SkyMED image with the EO-ALI medium resolution image.



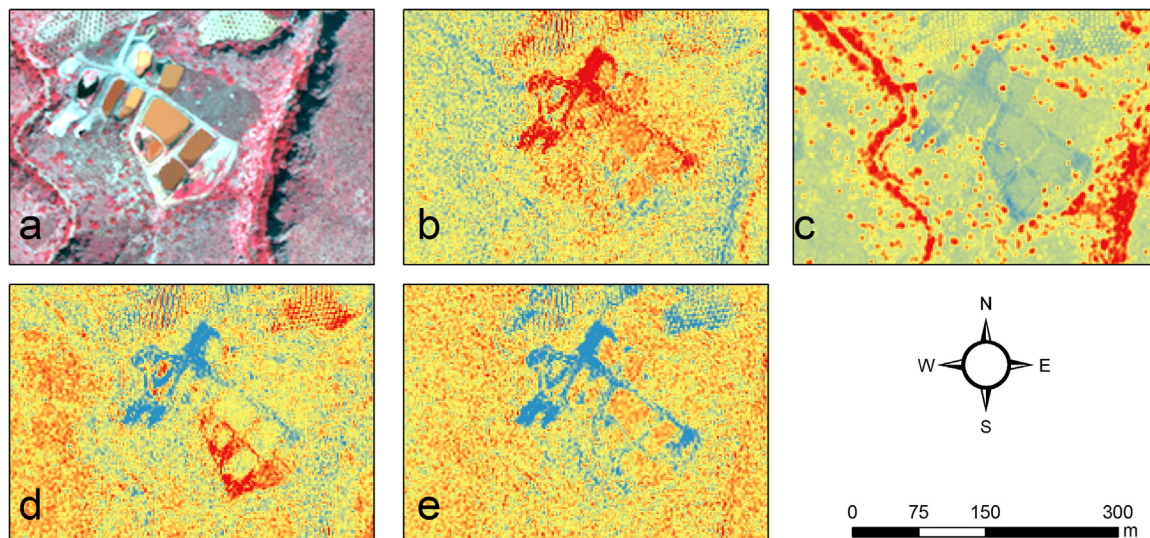


**Figure 8** Olive oil waste disposal area using the WorldView-2 image (05/03/2013) (a) after the application of the LSU (b) abundance maps for olive oil waste disposal areas; (c) abundance maps for vegetated areas; (d) abundance maps for white soil and (e) abundance maps for dark soils. Red colour indicates higher abundance for each endmember while blue colours lower values.

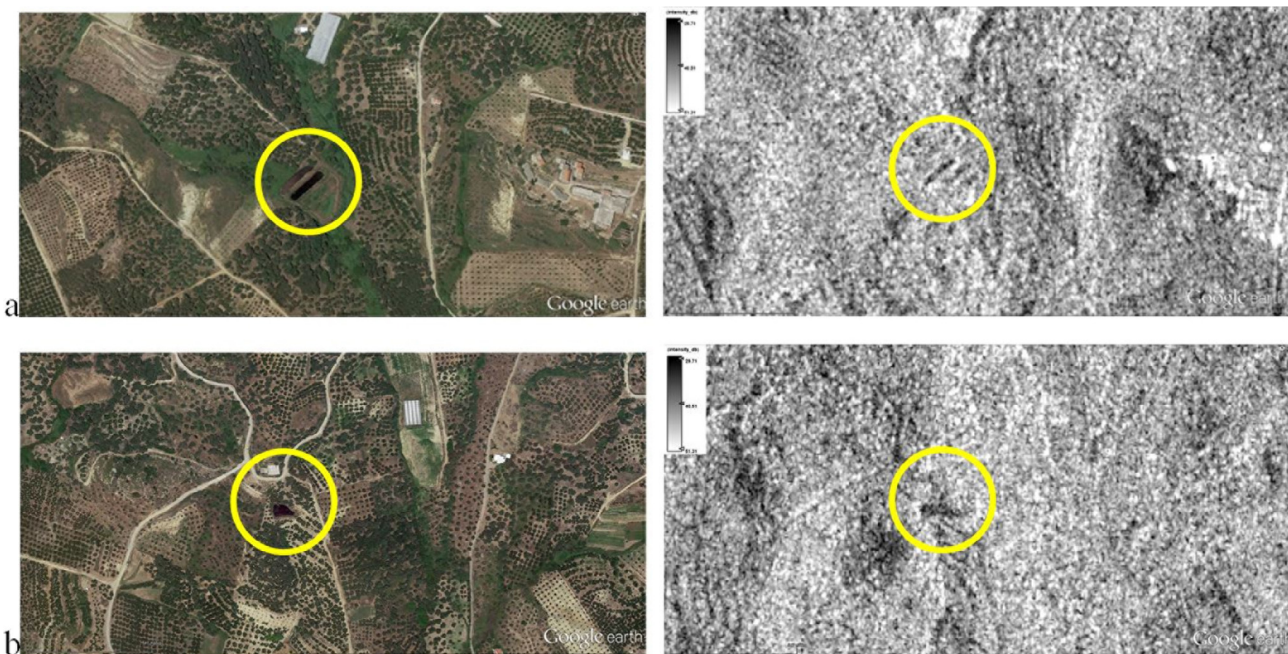


**Figure 9** Olive oil waste disposal area using the COSMO-SkyMed radar image (right). Left images indicate the two known olive oil waste disposal areas as seen in Google Earth.

However, in general as it was demonstrated in this study, well known algorithms such as NDVI, PCA and IHS transformation can be sufficiently used to identify OOWM disposal areas. The most promising results were generated after the application of the PCA analysis (specially the 1st principal component) and the IHS transformation while unsupervised classification and OOWM also provided satisfactory results.

Unsupervised classification applied for Pleiades image has indicated that the automatic extraction of OOWM disposal areas might be feasible. Indeed, the OOWM disposal areas were able to be detected quite clearly due to the unique spectral

profile of the targets (see Agapiou et al. (in press)). Since the majority of olive oil production on an international level is mainly limited in Mediterranean countries, where cloud cover is limited to just a few days, optical remote sensing can be used in a systematic way for the detection and monitoring of the OOWM disposal areas.

Despite the success of the passive optical sensors, an active sensor was also experimented in this study. The preliminary results from the COSMO-SkyMed radar image have indicated some potential for the detection of OOWM disposal areas which needs to be further studied and analysed.

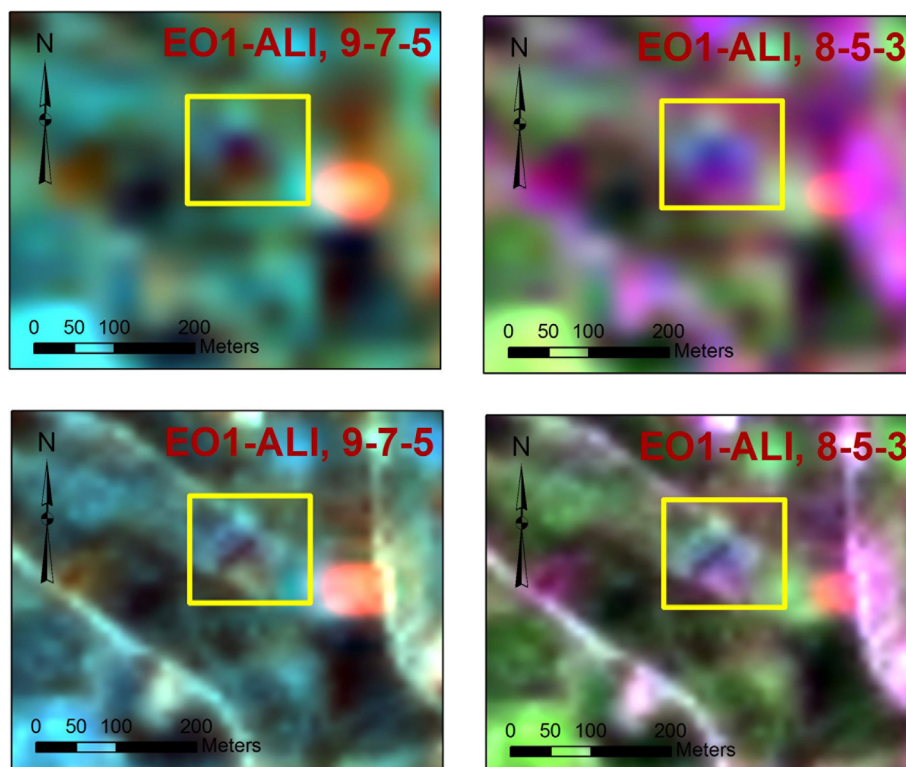


**Figure 10** False composites 9-7-5 and 8-5-3 from EO-ALI image before (top) and after (bottom) the fusion with the COSMO-SKyMed image.

## 5. Conclusion

Remote sensing techniques have been widely used as a tool for systematic monitoring of the environment (Rayegani et al., 2016; Butt et al., 2015). Remote sensing may provide additional advantages compared to in situ observations including the cost. OOMW disposal areas remain a critical environmental problem for the island of Crete and beyond. The huge quantities of wastes produced every year from oil extraction, scattered in the whole island need to be systematically monitored. In situ observation and recording of all OOMW disposal areas need to be supported by other alternative ways. In this direction, the aim of this paper was to evaluate and assess a variety of remote sensing datasets and algorithms for the detection of disposal areas.

Previous studies carried out by Alexakis et al. (2016) have shown that medium resolution satellite datasets such as Landsat may be able to detect OOMW disposal areas after the application of image analysis techniques. Nevertheless some problems were recorded regarding the detection of small OOMW disposal areas. These problems are linked with the spatial resolution of the images. Indeed, as Agapiou et al. (2015b) argue satellite data with higher spatial resolution are very effective for the detection of OOMW disposal areas. Although this study exploits only a limited number of some currently active satellite sensors, the results from where found very promising. The overall results have shown that a semi-automatic procedure for the exposure of OOMW disposal areas is feasible.

In this study, an attempt to further examine the potential use of remote sensing datasets and methodologies for the discovery of such disposal areas was carried out. Indeed, it was found that new satellite sensors with higher spatial resolution may be used as tools for systematic monitoring of the environment. Some of the most promising satellite datasets (i.e. with high spatial resolution) that exist today such as Pleiades (0.50 m), SPOT 6 (1.5 m), QuickBird (0.60 m), WorldView-2 (0.40 m) and GeoEye 1 (0.40 m) sensors covering central Crete were mainly employed. Several OOMW disposal areas were able to be detected using either simple (e.g. NDVI, OOMW indices) or more complicated (e.g. LSU) image processing techniques.

The overall analysis indicates that remote sensing satellite images can be efficiently used to map and monitor OOMW disposal areas. Indeed, remote sensing data can provide a cost effective way to detect both legal as well as illegal OOMW open air disposal areas. In a further time scale, this information can be imported into a GIS based geodatabase to document the whole cycle of olive oil production. While radar images are relatively recently used in a systematic way for detection and mapping of land use areas, mainly due to the high cost of such images, the free exploitation of the new sensors such as Sentinel-1 will further drive knowledge to this direction. Further work is expected to be carried out by the authors in the near future using high resolution hyperspectral airborne measurements. Such datasets may be examined so as to move a step forwards so as to correlate the spectral signatures of the wastes with specific pollutant types. For this to

be achieved chemical analysis and sampling of the wastes are necessary.

### Acknowledgment

This work was performed in the framework of the PEFYKA project within the KRIPIS Action of the GSRT. The project is funded by Greece and the European Regional Development Fund of the European Union under the NSRF and the O.P. Competitiveness and Entrepreneurship.

### References

- Agapiou, A., Hadjimitsis, D.G., Alexakis, D.D., 2012. Evaluation of broadband and narrowband vegetation indices for the identification of archaeological crop marks. *Remote Sensing* 4 (12), 3892–3919. <http://dx.doi.org/10.3390/rs4123892>.
- Agapiou, A., Papadopoulos, N., Sarris, A., 2015. Discriminant analysis of olive oil mill wastes using spectroradiometers in the visible and near infrared part of the spectrum. *Eur. J. Remote Sensing* 48, 793–809. <http://dx.doi.org/10.5721/EuJRS20154844>.
- Agapiou, A., Papadopoulos, N., Sarris, A., in press. Detection of olive oil mill waste (OOMW) disposal areas in the island of Crete using freely distributed high resolution GeoEye's OrbView-3 and Google Earth images. *Open GeoScience*.
- Alexakis, D.D., Sarris, A., Kalaitzidis, C., Papadopoulos, N., Soupios, P., 2016. Integrated use of satellite remote sensing, GIS and ground spectroscopy techniques for monitoring olive oil mill waste disposal areas in Crete Island-Greece. *Int. J. Remote Sens.* 37 (3), 669–693. <http://dx.doi.org/10.1080/01431161.2015.1136444>.
- Asfi, M., Ouzounidou, G., Panajiotidis, S., Therios, I., Moustakas, M., 2012. Toxicity effects of olive-mill wastewater on growth, photosynthesis and pollen morphology of spinach plants. *Ecotoxicol. Environ. Saf.* 80 (1), 69–75.
- Bailey, A.R., Clark, M.H., Ferris, P.J., Krause, S., Strong, L.R., 2002. Solid waste disposal and recycling. In: Bailey, Ronald A., Clark, Herbert M., Ferris, James P., Krause, Sonja., Strong, Robert L. (Eds.), *Chemistry of the Environment*, second ed. Academic Press, San Diego, pp. 769–792, 2002.
- Butt, A., Shabbir, R., Ahmad, S.S., Aziz, N., 2015. Land use change mapping and analysis using remote sensing and GIS: a case study of Simly watershed, Islamabad, Pakistan. *Egypt. J. Remote Sensing Space Sci.* 18 (2), 251–259.
- Camarsa, G., Gardner, S., Jones, W., Eldridge, J., Hudson, T., Thorpe, E., Hara, E., 2010. Good Practice in Improving Environmental Performance in the Olive OIL SECTOR. Office for Official Publications of the European Union, Luxembourg.
- Campbell, J.B., 2007. *Introduction to Remote Sensing*, fourth ed. The Guilford Press, ISBN-13: 978-1609181765.
- Dellagrecia, M., Monaco, P., Pinto, G., Pollio, A., Previtera, L., Temussi, F., 2001. Phytotoxicity of low-molecular-weight phenols from olive mill wastewaters. *Bull. Environ. Contam. Toxicol.* 67, 352–359.
- Dermeche, S., Nadour, M., Larroche, C., Moulti-Mati, F., Michaud, P., 2013. Olive mill wastes: biochemical characterizations and valorization strategies. *Process Biochem.* 48 (10), 1532–1552. <http://dx.doi.org/10.1016/j.procbio.2013.07.010>, ISSN 1359–5113.
- Doula, M.K., Tinivella, F., Sarris, A., Kavvadias, V., Moreno, Ortego J., Komnitsas, K., 2014. Agricultural wastes: protecting soil quality by sustainable disposal and reuse in agriculture. In: Zorbas, Antonis (Ed.), *Sustainability behind Sustainability*. Nova Science Publishers, pp. 243–274, Social Issues, Justice and Status.
- El-Asmar, M.H., Hereher, E.M., El Kafrawy, B.S., 2013. Surface area change detection of the Burullus Lagoon, North of the Nile Delta, Egypt, using water indices: a remote sensing approach. *Egypt. J. Remote Sensing Space Sci.* 16 (1), 119–123.
- Hegazy, M.N., Effat, H.A., 2010. Monitoring some environmental impacts of oil industry on coastal zone using different remotely sensed data. *Egypt. J. Remote Sensing Space Sci.* 13 (1), 63–74.
- Hegazy, I.R., Kaloop, R.M., 2015. Monitoring urban growth and land use change detection with GIS and remote sensing techniques in Daqahlia governorate Egypt. *Int. J. Sustainable Built Environ.* 4 (1), 117–124.
- International Olive Council, < <http://www.internationaloliveoil.org> >.
- Paredes, M.J., Moreno, E., Ramos-Cormenzana, A., Martinez, J., 1987. Characteristics of soil after pollution with wastewaters from olive oil extraction plants. *Chemosphere* 16 (7), 1557–1564.
- Pavlidou, A., Anastasopoulou, E., Dassenakis, M., Hatzianestis, I., Paraskevopoulou, V., Simbora, N., Rousselaki, E., Drakopoulou, P., 2014. Effects of olive oil wastes on river basins and an oligotrophic coastal marine ecosystem: a case study in Greece. *Sci. Total Environ.* 497–498 (1), 38–49.
- Peikert, B., Schaumann, G.E., Keren, Y., Bukhanovsky, N., Borisover, M., Garfha, M.A., Shoeric, J.H., Dag, A., 2015. Characterization of topsoils subjected to poorly controlled olive oil mill wastewater pollution in West Bank and Israel. *Agric. Ecosyst. Environ.* 199 (1), 176–189.
- Rawat, J.S., Kumar, M., 2015. Monitoring land use/cover change using remote sensing and GIS techniques: a case study of Hawalbagh block, district Almora, Uttarakhand, India. *Egypt. J. Remote Sensing Space Sci.* 18 (1), 77–84.
- Rayegani, B., Barati, S., Alsadat, T., Sonboli, B.S., 2016. Remotely sensed data capacities to assess soil degradation. *Egypt. J. Remote Sensing Space Sci.* <http://dx.doi.org/10.1016/j.ejrs.2015.12.001>. Available online 7 January 2016, ISSN 1110-9823.
- Rodis, P.S., Karathanos, V.T., Mantzavinou, A., 2002. Partitioning of olive oil antioxidants between oil and water phases. *J. Agric. Food Chem.* 2002 (50), 596–601.
- Roig, A., Cayuela, M.L., Sánchez-monedero, M.A., 2006. An overview on olive mill wastes and their valorisation methods. *Waste Manage.* 26 (9), 960–969.
- Tu, T.-M., Su, S.-C., Shyu, H.C., Huang, P.S., 2001. Efficient intensity-hue-saturation-based image fusion with saturation compensation. *Opt. Eng.* 40 (5), 720–728.
- Zhang, Y., Gao, J., Liu, L., Wang, Z., Ding, M., Yang, X., 2013. NDVI-based vegetation changes and their responses to climate change from 1982 to 2011: a case study in the Koshi River Basin in the middle Himalayas. *Global Planet. Change* 108, 139–148.